Operando Spectroscopy

International Edition: DOI: 10.1002/anie.201908871
German Edition: DOI: 10.1002/ange.201908871

Elucidating the Mechanism of Working SnO_2 Gas Sensors Using Combined Operando UV/Vis, Raman, and IR Spectroscopy

*Ann-Kathrin Elger and Christian Hess**

Abstract: *SnO_2 is the most widely used metal oxide gas-sensing material but a detailed understanding of its functioning is still lacking despite its relevance for applications. To gain new mechanistic insight into SnO_2 gas sensors under working conditions, we have developed an operando approach based on combined UV/Vis, Raman, and FTIR spectroscopy, allowing us for the first time to relate the sensor response to the concentration of oxygen vacancies in the metal oxide, the nature of the adsorbates, and the gas-phase composition. We demonstrate with the example of ethanol gas sensing that the sensor resistance is directly correlated with the number of surface oxygen vacancies and the presence of surface species, in particular, acetate and hydroxy groups. Our operando results enable an assessment of mechanistic models proposed in the literature to explain gas sensor operation. Owing to their fundamental nature, our findings are of direct relevance also for other metal oxide gas sensors.*

Metal oxide semiconductors, for example, SnO_2, have attracted a great deal of attention in the context of gas-sensing applications because of their high sensitivity and simple fabrication.[1–3] Their basic principle of operation is the monitoring of changes in the electrical conductivity, which are induced by the adsorption of target molecules on the semiconductor's surface. For a detailed understanding of their functioning, necessary in the rational design of better gas sensors, the identification of the gas-sensing mechanism is crucial, but monitoring the gas-induced surface processes and their relation to the sensors' conductivity changes remains a tremendous challenge.[4–6] To facilitate the knowledge-based design of gas sensors, operando approaches have been developed based on IR, Raman, UV/Vis, and X-ray absorption spectroscopy,[6–12] enabling the sensor response to be related to its structural changes directly under working conditions. In these studies the influence of oxygen vacancies and hydroxy groups on the SnO_2 gas-sensing behavior has been proposed, but no direct correlation between structure and activity was established.[7,11] Previous operando work has also revealed that owing to the complexity of metal oxide gas sensors a combination of techniques is highly desirable to unravel their mode of operation. In this contribution, we present a new operando spectroscopic approach combining resistance measurements with three spectroscopic techniques (UV/Vis, Raman, Fourier transform infrared (FTIR)) in one experimental setup for the first time, as illustrated in the inset of Figure 1. In this multiple spectroscopic experiment, UV/Vis spectra are used to monitor the number of oxygen vacancies in SnO_2, Raman spectra reveal the presence of adsorbates and hydroxy groups, and simultaneously recorded FTIR spectra capture the gas-phase composition during ethanol (EtOH) gas sensing. By systematically varying the gas atmosphere and temperature, we can relate the SnO_2 sensor response to the multiple spectroscopic changes, enabling us to obtain new fundamental insight into the functioning of metal-oxide semiconductor gas sensors.

Figure 1a depicts typical reflectance spectra of the SnO_2 gas sensor at 325 °C in various gas environments. For details of the preparation and characterization of the SnO_2 gas sensor, and UV/Vis spectra at higher wavelengths (Figure S1) please refer to the Supporting Information. As has been shown previously, a decrease in reflectance in the visible range of SnO_2 is caused by increased sample absorption originating from the presence of oxygen vacancies, i.e., SnO_2 reduction.[13] In fact, Figure 1 shows that starting from the oxidized gas sensor (air), exposure to increasingly reducing gas environments (air→N_2→EtOH/air→EtOH/N_2) results in a systematic decrease in the reflectance as a result of increasing absorption in the visible, as indicated for example by the behavior at 525 nm (see dashed line). Note that the legend displays the order of the experiments from top to bottom. Upon switching to pure nitrogen flow after EtOH/N_2 exposure, the reflectance increases again (see green spectrum), but not to the original level (see red spectrum) due to limited oxygen availability as discussed below. Summarizing, the reflectance in the visible can be considered as a sensitive indicator of the level of reduction of the SnO_2 gas sensor.[9,14]

Figure 1b depicts visible Raman spectra of the SnO_2 gas sensor for different gas compositions at 190 °C (bottom spectra) and 325 °C (top spectra). For the corresponding low-frequency spectra please refer to Figure S2. Please note that the spectra are offset for clarity. Starting at the bottom, the spectrum of SnO_2 in nitrogen at 190 °C is characterized by Raman features at 3631 and 3660 cm^{-1}, originating from terminal hydroxy groups.[14] Detailed analysis reveals additional weak features at around 3550 cm^{-1} and 3720 cm^{-1}, which, based on previous work, may be attributed to bridging and terminal hydroxy groups, respectively.[14] Upon exposure

[*] A.-K. Elger, Prof. Dr. C. Hess
Eduard-Zintl-Institut für Anorganische und Physikalische Chemie
Technische Universität Darmstadt
Alarich-Weiss-Str. 8, 64287 Darmstadt (Germany)
E-mail: hess@pc.chemie.tu-darmstadt.de
Supporting information and the ORCID identification number(s) for the author(s) of this article can be found under: https://doi.org/10.1002/anie.201908871.

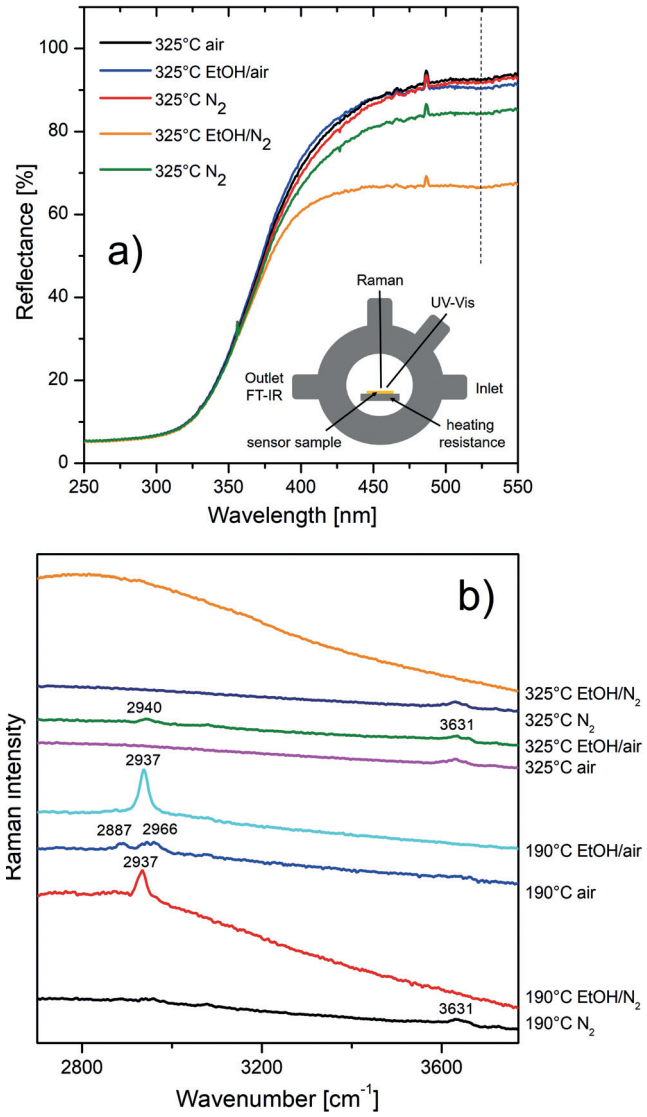

Figure 1. Operando spectra of the SnO_2 gas sensor. a) UV/Vis spectra at 325 °C showing the reflectance as a function of gas composition as indicated. The feature at 487 nm is an artifact of the spectrometer. The legend displays the order of the experiments from top to bottom. The inset shows a scheme of the multiple operando spectroscopic setup. b) Raman spectra at 514.5 nm excitation for various temperatures and gas compositions as indicated. Spectra are offset for clarity.

of the sample to EtOH, a new Raman band appears at 2937 cm^{-1}, whereas the hydroxy-related features are no longer observed. A similar behavior has previously been reported for In_2O_3 gas sensors,[6,15] and has been rationalized by the formation of acetate species ($\nu_{C\text{-}H}$) as a result of the reaction of (adsorbed) ethanol with surface hydroxy groups. Exposure to air results in a strong intensity decrease of the 2937 cm^{-1} band, which now appears as part of a broad feature centered around 2950 cm^{-1}. More detailed analysis reveals that this feature may be described by two contributions located at 2937 and 2966 cm^{-1}. In addition, a new Raman band appears at 2887 cm^{-1}, which in combination with the band at 2966 cm^{-1} is typical for the presence of formate ($\nu_{C\text{-}H}$),[15] thus indicating the partial decomposition of acetate into formate. Minor hydroxy-related features are observed at 3631 and 3660 cm^{-1}. Subsequent exposure to EtOH/air results in the disappearance of all Raman features except the acetate band at 2937 cm^{-1}, thus resembling the spectrum in $EtOH/N_2$.

Turning to the 325 °C spectra, the adsorbate ($\nu_{C\text{-}H}$) features are generally weaker because the surface processes are faster than at 190 °C. While the spectrum of SnO_2 in air is characterized by terminal hydroxy features at 3631 and 3660 cm^{-1}, upon exposure to EtOH, additionally, a small acetate band at 2940 cm^{-1} is observed. The absence of oxygen has a dramatic effect on the Raman spectra recorded in the presence of EtOH. Broad bands at 850–1650 cm^{-1} arising from carbon species are observed (see Figure S2), which originate from adsorbate decomposition. As a consequence of the presence of such a carbon overlayer, hydroxy- and/or adsorbate-related ($\nu_{C\text{-}H}$) Raman bands are no longer observable. In summary, the operando Raman spectra provide information on the presence of adsorbates and hydroxy groups during EtOH gas sensing that is characteristic for the respective temperature and gas composition.

Figure 2 depicts results of the simultaneous measurement of the sensor resistance, the reflectance (at 525 nm), Raman band intensities, and FTIR spectra of the gas-phase products. As will be discussed in detail in the following, this data set can be used to reveal correlations of the sensor resistance with the spectroscopic features. The assignment of the IR gas-phase bands is summarized in Table 1.

As shown in Figure 2, switching the gas atmosphere from nitrogen to 250 ppm $EtOH/N_2$ at 190 °C leads to a strong resistance decrease owing to a release of electrons into the conduction band, as expected for an n-type semiconductor gas sensor exposed to a reducing gas. As reaction products, carbon dioxide, acetaldehyde, and water (not shown) were detected, and the concentrations were quantified by means of calibration curves. The formation of acetaldehyde has previously been proposed to proceed via adsorbed ethoxy undergoing dehydrogenation.[15,16] During exposure of the gas sensor to $EtOH/N_2$, the reflectance decreases from 100 % to 84 % as a result of oxygen-vacancy formation, i.e., SnO_2 reduction.[13] Besides, as shown at the bottom of Figure 2, Raman data reveals the formation of acetate species resulting from the reaction of (adsorbed) ethanol with surface hydroxy groups as discussed in the context of Figure 1. Note that the Raman band intensities in Figure 2 were obtained on the basis of Raman spectra recorded over 10 min (as indicated by the bars), whereas the UV/Vis spectra were taken within 1 min directly after the Raman spectra. Switching back to pure nitrogen induces a small increase in the resistance and in the reflectance (to 85 %), whereas the acetate Raman band exhibits a small intensity decrease. Consistent with this behavior, the IR gas-phase signal shows that there is CO_2 desorption from the sensor surface, indicating the decomposition of part of the acetate species. The behavior of the resistance and the Raman features in nitrogen resembles that observed previously for ethanol gas sensing on In_2O_3, which has been attributed to the presence of stable acetate adsorbates formed during $EtOH/N_2$ exposure, preventing the sensor from returning to its initial state.[6,15]

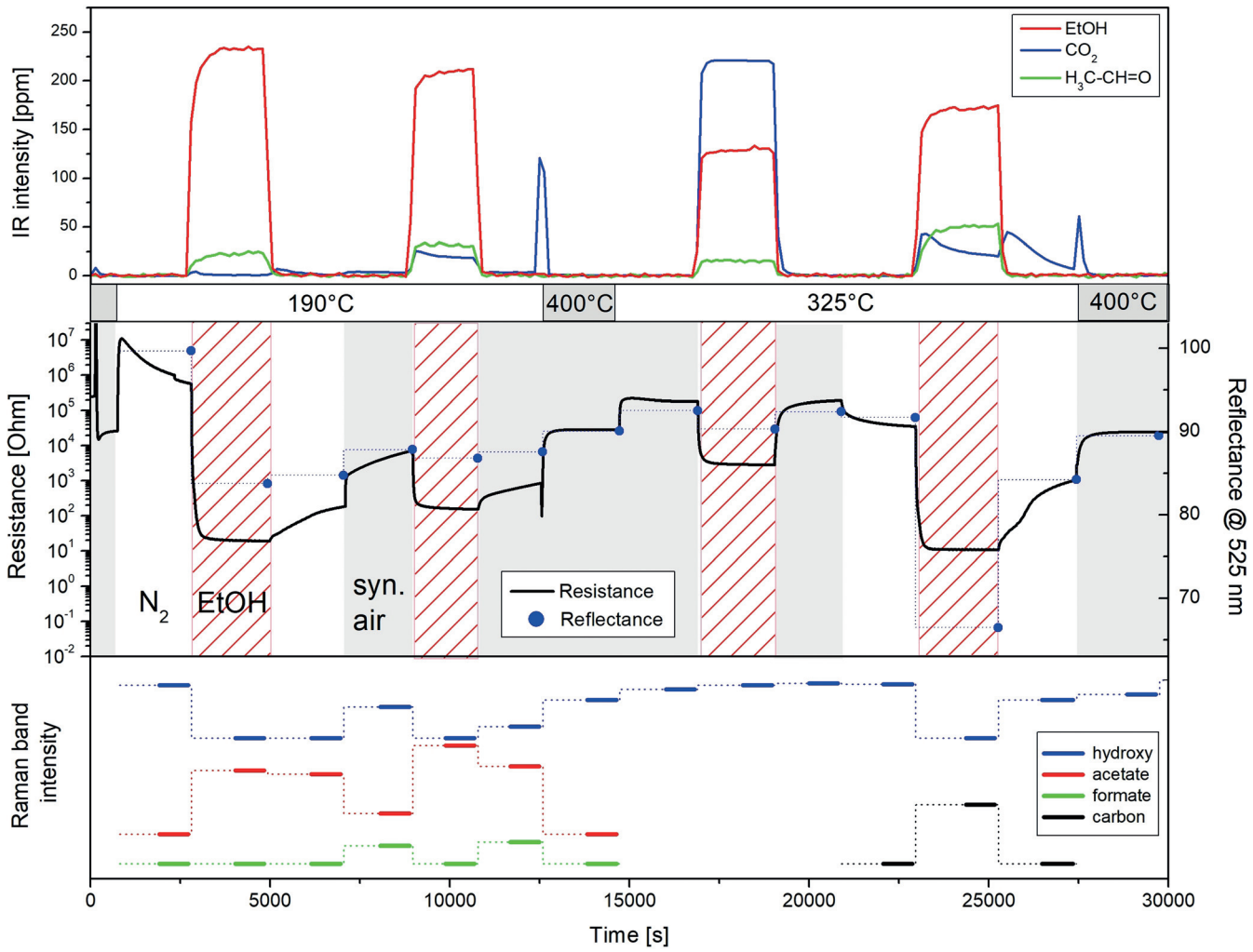

Figure 2. Temporal correlation of spectroscopic data and sensor resistance of the combined operando UV/Vis, Raman, and IR experiment during ethanol gas sensing of SnO_2. Dashed lines are a guide to the eye. Raman band intensities of hydroxy and acetate species are offset for clarity. For details see text.

Table 1: Assignment of the IR gas-phase bands of ethanol (EtOH), carbon dioxide (CO_2), and acetaldehyde ($H_3C{-}CH{=}O$) used for the correlation in Figure 2.

Wavenumber [cm^{-1}]	Gas
2903	EtOH
2361	CO_2
2733	$H_3C{-}CH{=}O$

When oxygen is added, first a prompt and then a slower increase of the sensor resistance is observed, which can be explained by the reoxidation of the sensor surface, removing electrons from the conduction band. Spectroscopic evidence for the surface reoxidation is provided by UV/Vis spectroscopy showing an increase of the reflectance (to 88%) and by Raman spectra exhibiting a decrease in the acetate and an increase in the formate signal, thus indicating the partial decomposition of acetate into formate; moreover, the presence of CO_2 in the gas phase confirms that part of the acetate is fully oxidized. Upon exposure to 250 ppm ethanol in air, the sensor shows a decrease in resistance. Note that the resistance decrease is less pronounced than in $EtOH/N_2$ as the presence of oxygen allows for permanent reoxidation. This is in agreement with the observed decrease in reflectance (to 87%), confirming an overall smaller degree of reduction of the gas sensor. Analysis of the Raman data reveals the formation of acetate species by consumption of surface hydroxy groups, as discussed above. As reaction products, acetaldehyde, carbon dioxide, and water were observed. From Figure 2 it is evident that the main product, carbon dioxide, was formed at a higher rate than in $EtOH/N_2$, resulting in a higher conversion of EtOH. Switching back to air leads to an immediate increase in resistance followed by a slower continuous increase, which is attributed to the reoxidation of the surface, as evidenced by the increase in reflectance to 88%, the partial decomposition of acetate to formate, and the presence of a gas-phase CO_2 signal.

Prior to the experiments at 325 °C, the SnO_2 sensor was heated to 400 °C to remove all adsorbates from the surface. Decomposition and/or desorption of the remaining adsorbates by thermal decomposition results in the formation of a sharp CO_2 signal, as identified by FTIR spectroscopy. As

a result of adsorbate decomposition, the resistance shows an increase when the sensor is heated to 400 °C in air, returning to its initial value before the 190 °C experiments; likewise, the reflectance and the Raman adsorbate intensities return to their starting values.

A temperature decrease to 325 °C resulted in an increase in resistance, again in agreement with normal semiconductor behavior. When switching to 250 ppm ethanol in air at 325 °C, a significantly higher CO_2 concentration was observed than at 190 °C, while acetaldehyde showed a similar concentration. The resistance showed a small decrease, which returned to its value before EtOH exposure when the feed was switched back to air. Following the resistance behavior, the reflectance first decreased from 93 % to 90 % in EtOH/air and then returned to 93 % in air. Under these conditions, no adsorbates are detected by Raman spectroscopy, consistent with the faster product formation at 325 °C. Switching the feed from air to nitrogen leads to a minor decrease of the resistance accompanied by a small decrease in reflectance to 92 %, consistent with an increase in the concentration of oxygen vacancies.

Upon exposure to 250 ppm EtOH/N_2 at 325 °C, the resistance showed a decrease, which is significantly stronger than in EtOH/air owing to the missing reoxidation of the SnO_2 sensor by oxygen. In comparison to ethanol in air at 325 °C, a smaller ethanol conversion and a significantly larger fraction of acetaldehyde is detected, besides CO_2 and water, reflecting the decreased availability of oxygen at the surface. The oxygen deficiency of the gas sensor is also evident from the reflectance behavior, showing a strong decrease from 91 % to 67 %. Under these reducing conditions, new Raman bands appear at around 1350 cm^{-1} and 1575 cm^{-1}, which have been assigned to the D and G bands of carbon, respectively, indicating the decomposition of ethanol on the sensor surface (see Figure S2). As discussed above, because of the presence of carbon, hydroxy- and/or adsorbate-related ($\nu_{C\text{-}H}$) Raman bands can no longer be detected. Also, carbon species are expected to contribute to the strong decrease in reflectance.

When the feed was switched back to pure nitrogen, the resistance increased not as fast as in the presence of oxygen at 325 °C but faster than at 190 °C. The changes caused by exposure to ethanol were largely reversible in the UV/Vis and Raman spectra. The reflectance increased to 84 %, and the Raman bands related to deposited surface carbon disappear, while those related to hydroxy groups reappear. The observed behavior indicates that at 325 °C, in contrast to the behavior at 190 °C, oxygen diffusion processes from the bulk to the surface are fast enough to allow for reoxidation of the sensor and oxidation of residual carbon. As a consequence, CO_2 is observed as a reaction product in the gas phase via IR spectroscopy (see Figure 2). This underlines the importance of simultaneous gas-phase analysis enabling the detection of adsorbates, present in concentrations below the Raman detection limit, undergoing surface reactions.

Finally, when oxygen was introduced, the resistance increased at once to the initial state in synthetic air caused by fast reoxidation of the surface, leading to removal of electrons from the conduction band. The surface reoxidation is spectroscopically evidenced by the increase in reflectance to 90 %. It is further accompanied by the decomposition and oxidation of adsorbates, resulting in a strong but narrow CO_2 signal. The smaller area as compared to the corresponding CO_2 signal at 190 °C can be rationalized by the higher conversion and therefore smaller number of adsorbates present at the surface at higher sensor temperature.

According to the gas-sensing mechanisms proposed in the literature, the sensor response can be explained by changes of the electric surface potential resulting from "ionosorption" of gaseous molecules (ionosorption model) or by changes in the oxygen stoichiometry, that is, by the variation of the number of (sub-)surface oxygen vacancies and their ionization (reduction–reoxidation mechanism), but direct mechanistic evidence is still scarce. Here we demonstrate with the example of a SnO_2 gas sensor used for ethanol gas sensing that the sensor response is correlated with the number of oxygen vacancies, the nature of the adsorbates, and the presence of surface hydroxy groups. This is illustrated in Figure 3, which depicts the reflectance and Raman band intensities of hydroxy and acetate species as a function of sensor resistance, together with least-squares fits to the experimental data from Figure 2.

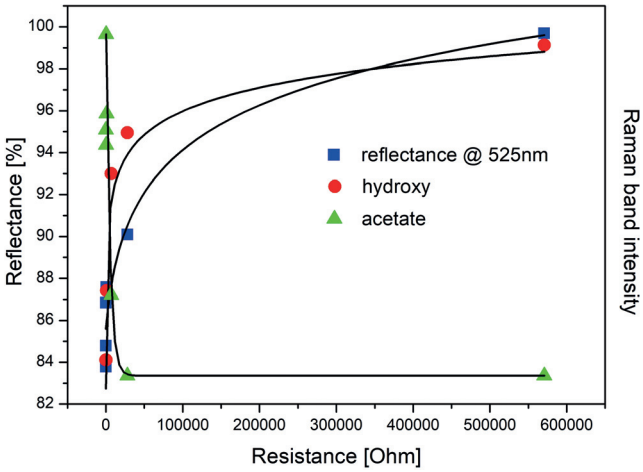

Figure 3. Reflectance and Raman band intensities of hydroxy and acetate species as a function of sensor resistance, together with least-squares fits to the experimental data from Figure 2.

Figure 3 shows that the resistance decreases as the number of oxygen vacancies and the formation of adsorbed acetate increases, which in turn is related to the consumption of hydroxy species. A dependence of the sensor response on the presence of adsorbates has been reported previously for In_2O_3 gas sensors,[6] from which an increase in acetate concentration leads to a decrease in resistance, fully consistent with the behavior observed here. Thus, our results show that ionosorption is of more general importance in (ethanol) gas sensing. Moreover, we demonstrate for the first time under operando gas-sensing conditions that the resistance is directly correlated with the concentration of oxygen vacancies. Further specification of their location has become feasible by recent Raman studies on ceria-based gas sensors reporting that the subsurface oxygen

vacancy dynamics is not relevant for gas sensing.[17,18] Transferring this knowledge to SnO_2 gas sensors thus strongly suggests that the correlation between resistance and reflectance observed in the present study can be attributed to oxygen vacancies located at the surface of the sensor. Our results demonstrate that operando Raman und UV/Vis spectroscopy are highly sensitive to structural changes of the metal oxide gas sensor material. Previous studies have revealed the potential of X-ray based methods to explore the state of metal dopants and potential electrode contributions,[8,10,12] as well as that of IR spectroscopy to probe the effect of humidity.[11] With the available techniques we may envision important aspects of technical semiconductor gas sensors to be monitored under working conditions in the near future.

Summarizing, we provide new insight into the mode of operation of widely used SnO_2 gas sensors, showing the relation of the sensor response to the number of surface oxygen vacancies and the nature of the adsorbates using a new multiple operando spectroscopic setup. Our findings are expected to be of direct relevance also for other metal oxide gas sensors and underline the importance of developing new operando approaches to enable a detailed spectroscopic analysis under working conditions.

Acknowledgements

This work was supported by the Deutsche Forschungsgemeinschaft (DFG, HE-4515/6-1). We thank Silvio Heinschke for performing nitrogen adsorption/desorption experiments, Kathrin Hofmann for XRD experiments, and Karl Kopp for XPS analysis and technical support.

Conflict of interest

The authors declare no conflict of interest.

Keywords: ethanol · gas sensors · mechanisms · operando spectroscopy · SnO_2

How to cite: *Angew. Chem. Int. Ed.* **2019**, *58*, 15057–15061
Angew. Chem. **2019**, *131*, 15199–15204

[1] D. E. Williams, *Sens. Actuators B* **1999**, *57*, 1–16.
[2] G. Korotcenkov, *Mater. Sci. Eng. B* **2007**, *139*, 1–23.
[3] A. Dey, *Mater. Sci. Eng. B* **2018**, *229*, 206–217.
[4] A. Gurlo, R. Riedel, *Angew. Chem. Int. Ed.* **2007**, *46*, 3826–3848; *Angew. Chem.* **2007**, *119*, 3900–3923.
[5] N. Barsan, D. Koziej, U. Weimar, *Sens. Actuators B* **2007**, *121*, 18–35.
[6] S. Sänze, A. Gurlo, C. Hess, *Angew. Chem. Int. Ed.* **2013**, *52*, 3607–3610; *Angew. Chem.* **2013**, *125*, 3694–3698.
[7] D. Degler, S. Wicker, U. Weimar, N. Barsan, *J. Phys. Chem. C* **2015**, *119*, 11792–11799.
[8] D. Koziej, M. Hübner, N. Barsan, U. Weimar, M. Sikora, J.-D. Grunwaldt, *Phys. Chem. Chem. Phys.* **2009**, *11*, 8620–8625.
[9] D. Degler, N. Barz, U. Dettinger, H. Peisert, T. Chasse, U. Weimar, N. Barsan, *Sens. Actuators B* **2016**, *224*, 256–259.
[10] M. Hübner, D. Koziej, M. Bauer, N. Barsan, K. Kvashnina, M. D. Rossell, U. Weimar, J.-D. Grunwaldt, *Angew. Chem. Int. Ed.* **2011**, *50*, 2841–2844; *Angew. Chem.* **2011**, *123*, 2893–2896.
[11] S. Wicker, M. Guiltat, U. Weimar, A. Hémeryck, N. Barsan, *J. Phys. Chem. C* **2017**, *121*, 25064–25073.
[12] A. Gurlo, R. Riedel, *ChemPhysChem* **2010**, *11*, 79–82.
[13] D. Amalric Popescu, J.-M. Herrmann, A. Ensuque, F. Bozon-Verduraz, *Phys. Chem. Chem. Phys.* **2001**, *3*, 2522–2530.
[14] D. Amalric-Popescu, F. Bozon-Verduraz, *Catal. Today* **2001**, *70*, 139–154.
[15] S. Sänze, C. Hess, *J. Phys. Chem. C* **2014**, *118*, 25603–25613.
[16] D. Kohl, *Sens. Actuators* **1989**, *18*, 71–113.
[17] A.-K. Elger, J. Baranyai, K. Hofmann, C. Hess, *ACS Sens.* **2019**, *4*, 1497–1501.
[18] Note that the application of Raman spectroscopy, as discussed in Ref. [17], is limited to ceria materials. However, the use of UV/Vis spectroscopy, as presented here, enables a more general approach to access the relevant surface oxygen vacancies.

Manuscript received: July 16, 2019
Accepted manuscript online: August 26, 2019
Version of record online: September 12, 2019

